Chapter 3

Method Description and Implementation

This chapter discusses the implementation and solution of the LDO equations in Denovo, the parallel discrete ordinates radiation transport code package in the Exnihilo code suite [1]. First, a comparison of the traditional formulation of the discrete ordinates equations with the LDO equations is presented to demonstrate the difference in implementing the two separate sets of equations. Then, a brief discussion of scattering is given to highlight the specific differences between the two sets of equations with respect to how scattering is handled from the perspective of implementation. Following that is an overview of the quadrature sets used in solving the LDO equations in Denovo. Finally, we list and discuss the restrictions of using the LDO equations in combination with Exnihilo and ADVANTG for the purpose of Monte Carlo variance reduction parameter generation.

3.1 Operator Form

3.1.1 Traditional Discrete Ordinates Formulation

When considering deterministic methods, it is often instructive to think about the NTE in operator form. In accordance with the discretization in Section 2.1.2.1, the operator form of the traditional discrete ordinates equations [2] is

$$\mathbf{L}\Psi = \mathbf{MS}\Phi + Q, \tag{3.1}$$

$$\Phi = \mathbf{D}\Psi \text{ where } \mathbf{D} = \mathbf{M}^{\top}\mathbf{W}, \tag{3.2}$$

$$\left(\mathbf{I} - \mathbf{DL}^{-1}\mathbf{MS}\right)\Phi = \mathbf{DL}^{-1}Q. \tag{3.3}$$

The operators will be defined below, with the exception of $\mathbf{L}$, the transport operator. When solving Equation 3.3, the operation $\mathbf{L}^{-1}$ is referred to as a "sweep"; $\mathbf{L}$ is implicitly formed as a lower-left triangular matrix and is inverted by "sweeping" through the spatial mesh in the

direction of particle flow [2]. With this formulation, at each spatial unknown, with energy groups defined over the range $g \in [0, G-1]$ as described previously, we can write

$$\mathbf{L}\begin{pmatrix}\Psi_0\\ \Psi_1\\ \vdots\\ \Psi_{G-1}\end{pmatrix} = \begin{pmatrix}[\mathbf{M}] & 0 & 0 & 0\\ 0 & [\mathbf{M}] & 0 & 0\\ 0 & 0 & \ddots & \vdots\\ 0 & 0 & \cdots & [\mathbf{M}]\end{pmatrix}\begin{pmatrix}[\mathbf{S}]_{0\to 0} & [\mathbf{S}]_{1\to 0} & \cdots & [\mathbf{S}]_{G-1\to 0}\\ [\mathbf{S}]_{0\to 1} & [\mathbf{S}]_{1\to 1} & \cdots & [\mathbf{S}]_{G-1\to 1}\\ \vdots & \vdots & \ddots & \vdots\\ [\mathbf{S}]_{0\to G-1} & [\mathbf{S}]_{1\to G-1} & \cdots & [\mathbf{S}]_{G-1\to G-1}\end{pmatrix}\begin{pmatrix}\Phi_0\\ \Phi_1\\ \vdots\\ \Phi_{G-1}\end{pmatrix} + \begin{pmatrix}Q_0\\ Q_1\\ \vdots\\ Q_{G-1}\end{pmatrix}, \tag{3.4}$$

where the notation $[\cdot]_g$ indicates a block matrix over all unknowns for a single group.

Here, the angular flux vector for group g over angles $1, \ldots, N$ is defined as

$$\Psi_g = \begin{pmatrix}\psi_1^g & \psi_2^g & \psi_3^g & \cdots \psi_N^g\end{pmatrix}^\top, \tag{3.5}$$

with the external source vector Q_g defined similarly. The operator $\mathbf{M}$ is the "moment-to-discrete" matrix and is used to project harmonic moments onto discrete angle space. It is defined as

$$[\mathbf{M}] = \begin{pmatrix}Y_{00}^e(\mathbf{\Omega}_1) & Y_{10}^e(\mathbf{\Omega}_1) & Y_{11}^o(\mathbf{\Omega}_1) & Y_{11}^e(\mathbf{\Omega}_1) & \cdots & Y_{PP}^o(\mathbf{\Omega}_1) & Y_{PP}^e(\mathbf{\Omega}_1)\\ Y_{00}^e(\mathbf{\Omega}_2) & Y_{10}^e(\mathbf{\Omega}_2) & Y_{11}^o(\mathbf{\Omega}_2) & Y_{11}^e(\mathbf{\Omega}_2) & \cdots & Y_{PP}^o(\mathbf{\Omega}_2) & Y_{PP}^e(\mathbf{\Omega}_2)\\ Y_{00}^e(\mathbf{\Omega}_3) & Y_{10}^e(\mathbf{\Omega}_3) & Y_{11}^o(\mathbf{\Omega}_3) & Y_{11}^e(\mathbf{\Omega}_3) & \cdots & Y_{PP}^o(\mathbf{\Omega}_3) & Y_{PP}^e(\mathbf{\Omega}_3)\\ \vdots & \vdots & \vdots & \vdots & \ddots & \vdots & \vdots\\ Y_{00}^e(\mathbf{\Omega}_N) & Y_{10}^e(\mathbf{\Omega}_N) & Y_{11}^o(\mathbf{\Omega}_N) & Y_{11}^e(\mathbf{\Omega}_N) & \cdots & Y_{PP}^o(\mathbf{\Omega}_N) & Y_{PP}^e(\mathbf{\Omega}_N)\end{pmatrix}. \tag{3.6}$$

Note that $[\mathbf{M}]$ is dependent only on angle and is therefore the same for each energy group. The operator $\mathbf{D}$ is the "discrete-to-moment" matrix; it is used to calculate the moments of the angular flux from discrete angular flux values. $\mathbf{D}$ is calculated as $\mathbf{M}^\top\mathbf{W}$, where $\mathbf{W}$ is a diagonal matrix of quadrature weights [2], and it is written as

$$[\mathbf{D}] = \begin{pmatrix} w_1 Y_{00}^e(\mathbf{\Omega}_1) & w_2 Y_{00}^e(\mathbf{\Omega}_2) & w_3 Y_{00}^e(\mathbf{\Omega}_3) & \cdots & w_N Y_{00}^e(\mathbf{\Omega}_N) \\ w_1 Y_{10}^e(\mathbf{\Omega}_1) & w_2 Y_{10}^e(\mathbf{\Omega}_2) & w_3 Y_{10}^e(\mathbf{\Omega}_3) & \cdots & w_N Y_{10}^e(\mathbf{\Omega}_N) \\ w_1 Y_{11}^o(\mathbf{\Omega}_1) & w_2 Y_{11}^o(\mathbf{\Omega}_2) & w_3 Y_{11}^o(\mathbf{\Omega}_3) & \cdots & w_N Y_{11}^o(\mathbf{\Omega}_N) \\ w_1 Y_{11}^e(\mathbf{\Omega}_1) & w_2 Y_{11}^e(\mathbf{\Omega}_2) & w_3 Y_{11}^e(\mathbf{\Omega}_3) & \cdots & w_N Y_{11}^e(\mathbf{\Omega}_N) \\ \vdots & \vdots & \vdots & \ddots & \vdots \\ w_1 Y_{PP}^o(\mathbf{\Omega}_1) & w_2 Y_{PP}^o(\mathbf{\Omega}_2) & w_3 Y_{PP}^o(\mathbf{\Omega}_3) & \cdots & w_N Y_{PP}^o(\mathbf{\Omega}_N) \\ w_1 Y_{PP}^e(\mathbf{\Omega}_1) & w_2 Y_{PP}^e(\mathbf{\Omega}_2) & w_3 Y_{PP}^e(\mathbf{\Omega}_3) & \cdots & w_N Y_{PP}^e(\mathbf{\Omega}_N) \end{pmatrix}. \tag{3.7}$$

Like [**M**], [**D**] is dependent only on angle and is the same for each energy group. The scattering cross section matrices are defined as

$$[\mathbf{S}]_{g' \to g} = \begin{pmatrix} \Sigma_{\mathrm{s},0}^{g' \to g} & 0 & 0 & 0 & 0 & 0 & 0 \\ 0 & \Sigma_{\mathrm{s},1}^{g' \to g} & 0 & 0 & 0 & 0 & 0 \\ 0 & 0 & \Sigma_{\mathrm{s},1}^{g' \to g} & 0 & 0 & 0 & 0 \\ 0 & 0 & 0 & \Sigma_{\mathrm{s},1}^{g' \to g} & 0 & 0 & 0 \\ 0 & 0 & 0 & 0 & \ddots & 0 & 0 \\ 0 & 0 & 0 & 0 & 0 & \Sigma_{\mathrm{s},P}^{g' \to g} & 0 \\ 0 & 0 & 0 & 0 & 0 & 0 & \Sigma_{\mathrm{s},P}^{g' \to g} \end{pmatrix}, \tag{3.8}$$

where these scattering cross section coefficient values come from data libraries based on experimental measurements. Finally, the flux moment vectors are defined as

$$\Phi_g = \begin{pmatrix} \phi_{00}^g & \phi_{10}^g & \vartheta_{11}^g & \phi_{11}^g & \phi_{20}^g & \cdots & \vartheta_{PP}^g & \phi_{PP}^g \end{pmatrix}^\top, \tag{3.9}$$

where the flux moments are evaluated as listed in Equation 2.18. As we will describe below in Section 3.1.4, the goal of solving the discrete ordinates equations is to solve for these flux moments and then use the flux moments to calculate the scalar flux. In summary, the traditional discrete ordinates discretizations are captured in the preceding matrices; they can be used to analyze behavior and performance and can be compared against other discretizations.

3.1.2 LDO Formulation

As discussed in Chapter 2, although the LDO equations are formally the same as the traditional discrete ordinates equations, there are several key differences between the sets of equations. Here we present and discuss the operator form of the LDO equations as a comparison to the operator form of the discrete ordinates equations shown above. The operator form of the LDO equations is

$$\mathbf{L}\Psi = \tilde{\mathbf{S}}\mathbf{J}\Psi + Q, \tag{3.10}$$

$$\left(\mathbf{I} - \mathbf{L^{-1}}\tilde{\mathbf{S}}\mathbf{J}\right)\Psi = \mathbf{L^{-1}}Q. \tag{3.11}$$

Letting $\mathbf{D} \equiv \mathbf{I}$ with $\mathbf{L^{-1}} = \mathbf{IL^{-1}} = \mathbf{DL^{-1}}$, we then have

$$\left(\mathbf{I} - \mathbf{DL^{-1}}\tilde{\mathbf{S}}\mathbf{J}\right)\Psi = \mathbf{DL^{-1}}Q. \tag{3.12}$$

Equation 3.12 is in the same form as Equation 3.3, so we can apply the same solution techniques to both sets of equations.

In contrast to Equation 3.3, however, Equation 3.12 contains the Lagrange interpolation matrix $\mathbf{J}$ rather than the moment-to-discrete operator $\mathbf{M}$, and $\tilde{\mathbf{S}}$ contains the new formulation of scattering cross sections specific to the LDO equations. Additionally, when solving the LDO equations, we are solving for the angular flux coefficients rather than flux moments. Now, at each spatial unknown, with energy groups again defined over the range $g \in [0, G-1]$, we have

$$\mathbf{L}\begin{pmatrix}\Psi_0\\ \Psi_1\\ \vdots\\ \Psi_{G-1}\end{pmatrix} = \begin{pmatrix} [\tilde{\mathbf{S}}]_{0\to0} & [\tilde{\mathbf{S}}]_{1\to0} & \cdots & [\tilde{\mathbf{S}}]_{G-1\to0}\\ [\tilde{\mathbf{S}}]_{0\to1} & [\tilde{\mathbf{S}}]_{1\to1} & \cdots & [\tilde{\mathbf{S}}]_{G-1\to1}\\ \vdots & \vdots & \ddots & \vdots\\ [\tilde{\mathbf{S}}]_{0\to G-1} & [\tilde{\mathbf{S}}]_{1\to G-1} & \cdots & [\tilde{\mathbf{S}}]_{G-1\to G-1}\end{pmatrix}\begin{pmatrix}[\mathbf{J}] & 0 & 0 & 0\\ 0 & [\mathbf{J}] & 0 & 0\\ 0 & 0 & \ddots & \vdots\\ 0 & 0 & \cdots & [\mathbf{J}]\end{pmatrix}\begin{pmatrix}\Psi_0\\ \Psi_1\\ \vdots\\ \Psi_{G-1}\end{pmatrix} + \begin{pmatrix}Q_0\\ Q_1\\ \vdots\\ Q_{G-1}\end{pmatrix}, \tag{3.13}$$

where the block matrix notation still holds. The angular flux coefficient vector and external source vector are formed as listed in Equation 3.5. The operator $[\mathbf{J}]$ performs the Lagrange interpolation. It is constructed as the inverse of the Gram matrix, $\mathbf{G}$, which is calculated as

$$\mathbf{G} = \begin{pmatrix} \sum_{\ell=0}^{L}\frac{2\ell+1}{4\pi}P_\ell(\mathbf{\Omega}_1\cdot\mathbf{\Omega}_1) & \sum_{\ell=0}^{L}\frac{2\ell+1}{4\pi}P_\ell(\mathbf{\Omega}_1\cdot\mathbf{\Omega}_2) & \cdots & \sum_{\ell=0}^{L}\frac{2\ell+1}{4\pi}P_\ell(\mathbf{\Omega}_1\cdot\mathbf{\Omega}_N)\\ \sum_{\ell=0}^{L}\frac{2\ell+1}{4\pi}P_\ell(\mathbf{\Omega}_2\cdot\mathbf{\Omega}_1) & \sum_{\ell=0}^{L}\frac{2\ell+1}{4\pi}P_\ell(\mathbf{\Omega}_2\cdot\mathbf{\Omega}_2) & \cdots & \sum_{\ell=0}^{L}\frac{2\ell+1}{4\pi}P_\ell(\mathbf{\Omega}_2\cdot\mathbf{\Omega}_N)\\ \vdots & \vdots & \ddots & \vdots\\ \sum_{\ell=0}^{L}\frac{2\ell+1}{4\pi}P_\ell(\mathbf{\Omega}_N\cdot\mathbf{\Omega}_1) & \sum_{\ell=0}^{L}\frac{2\ell+1}{4\pi}P_\ell(\mathbf{\Omega}_N\cdot\mathbf{\Omega}_2) & \cdots & \sum_{\ell=0}^{L}\frac{2\ell+1}{4\pi}P_\ell(\mathbf{\Omega}_N\cdot\mathbf{\Omega}_N)\end{pmatrix}. \tag{3.14}$$

Like [**M**] and [**D**] in the traditional discrete ordinates formulation, [**J**] depends only on angle and is the same for all energy groups. Finally, the new scattering cross section matrix is:

$$[\tilde{\mathbf{S}}]_{g'\to g} = \begin{pmatrix} \Sigma_{\mathrm{s,L}}^{g'\to g}(\mathbf{\Omega}_1\cdot\mathbf{\Omega}_1) & \Sigma_{\mathrm{s,L}}^{g'\to g}(\mathbf{\Omega}_1\cdot\mathbf{\Omega}_2) & \cdots & \Sigma_{\mathrm{s,L}}^{g'\to g}(\mathbf{\Omega}_1\cdot\mathbf{\Omega}_N) \\ \Sigma_{\mathrm{s,L}}^{g'\to g}(\mathbf{\Omega}_2\cdot\mathbf{\Omega}_1) & \Sigma_{\mathrm{s,L}}^{g'\to g}(\mathbf{\Omega}_2\cdot\mathbf{\Omega}_2) & \cdots & \Sigma_{\mathrm{s,L}}^{g'\to g}(\mathbf{\Omega}_2\cdot\mathbf{\Omega}_N) \\ \vdots & \vdots & \ddots & \vdots \\ \Sigma_{\mathrm{s,L}}^{g'\to g}(\mathbf{\Omega}_N\cdot\mathbf{\Omega}_1) & \Sigma_{\mathrm{s,L}}^{g'\to g}(\mathbf{\Omega}_N\cdot\mathbf{\Omega}_2) & \cdots & \Sigma_{\mathrm{s,L}}^{g'\to g}(\mathbf{\Omega}_N\cdot\mathbf{\Omega}_N) \end{pmatrix}, \tag{3.15}$$

where each element of $[\tilde{\mathbf{S}}]_{g'\to g}$ is calculated as

$$\Sigma_{\mathrm{s,L}}^{g'\to g}(\mathbf{\Omega}_n\cdot\mathbf{\Omega}_m) = \sum_{\ell=0}^{L}\frac{2\ell+1}{4\pi}\Sigma_{\mathrm{s},\ell}^{g'\to g}P_\ell(\mathbf{\Omega}_n\cdot\mathbf{\Omega}_m). \tag{3.16}$$

In Equation 3.16, $\Sigma_{\mathrm{s},\ell}^{g'\to g}$ are the same cross section coefficients that are stored in the traditional scattering matrix given in Equation 3.8. We again note that the operator **D** is replaced by the identity matrix in the LDO formulation; incorporation of the quadrature set weights in the LDO equations is discussed in Section 3.1.4. In the LDO formulation Equations 3.14 – 3.16, L, the order at which the scattering expansion is truncated, is arbitrary. However, values of $\Sigma_{\mathrm{s},\ell}^{g'\to g}$ must exist for all values of $\ell \in [0, L]$, so we typically set L equal to the same scattering expansion $\mathrm{P_N}$ order P in Equations 3.6 – 3.8. A more detailed comparison of scattering between the discrete ordinates formulation and the LDO formulation is given below in Section 3.2.1.

To recap, space and energy are handled in the same way between the two different formulations, while angular discretization and scattering are handled differently. The traditional discrete ordinates formulation uses the **M** and **D** operators to project harmonic moments onto discrete angle space and to calculate moments of the angular flux from discrete angular flux values, respectively. In contrast, the LDO formulation employs the interpolation matrix **J** and the scattering matrix $\tilde{\mathbf{S}}$ to capture angular information in the problem. We will look at the operator sizing for the two formulations in the next section to verify that these differences are compatible with respect to implementing the LDO equations in a software framework that was written to solve the discrete ordinates equations.

3.1.3 Operator Sizes

To evaluate the feasibility of constructing and solving the LDO equations in Denovo, it is pertinent to look at the dimensions of the operator forms of each equation. By doing this, we verify that the data structures for the discrete ordinates form can be leveraged to solve the LDO equations.

The sizes used for the discrete ordinates equations are

$$\begin{aligned}
G &= \text{number of energy groups,}\\
N &= \text{number of discrete angles,}\\
P &= \text{scattering expansion } P_N \text{ order,}\\
T &= (P+1)^2 = \text{number of flux moments,}\\
C &= \text{number of spatial cells,}\\
E &= \text{number of unknowns per spatial cell.}
\end{aligned}$$

Now, we define

$$a = G \times N \times C \times E \quad \text{and} \quad b = G \times T \times C \times E. \tag{3.17}$$

The operator sizes of the original formulation are then

$$\begin{aligned}
\mathbf{I} &= (a \times a);\\
\mathbf{D} &= (b \times a), \quad [\mathbf{D}] = (TCE \times NCE);\\
\mathbf{L} = \mathbf{L^{-1}} &= (a \times a);\\
\mathbf{M} &= (a \times b), \quad [\mathbf{M}] = (NCE \times TCE);\\
\mathbf{S} &= (b \times b), \quad [\mathbf{S}] = (TCE \times TCE);\\
\Phi &= (b \times 1), \quad \Phi_g = (TCE \times 1);\\
\Psi &= (a \times 1), \quad \Psi_g = (NCE \times 1);\\
Q &= (a \times 1), \quad Q_g = (NCE \times 1).
\end{aligned}$$

The sizes used in the LDO formulation are

$$\begin{aligned}
G &= \text{number of energy groups,}\\
H &= \text{degree of spherical harmonics subspace to integrate,}\\
N &= (H+1)^2 = \text{number of discrete angles,}\\
P &= \text{scattering expansion } P_N \text{ order,}\\
T &= (H+1)^2 = \text{number of angular flux coefficients,}\\
C &= \text{number of spatial cells,}\\
E &= \text{number of unknowns per spatial cell.}
\end{aligned}$$

Again, we define a and b as calculated in Equation 3.17. The operator sizes of the LDO formulation are then

$$\begin{aligned}
\mathbf{I} = \mathbf{D} &= (a \times a); \\
\mathbf{L} = \mathbf{L^{-1}} &= (a \times a); \\
\tilde{\mathbf{S}} &= (a \times a),\ [\tilde{\mathbf{S}}] = (NCE \times NCE); \\
\mathbf{J} &= (a \times a),\ [\mathbf{J}] = (NCE \times NCE); \\
\Psi &= (a \times 1),\ \Psi_g = (NCE \times 1); \\
Q &= (a \times 1),\ Q_g = (NCE \times 1).
\end{aligned}$$

In the LDO formulation, since the number of flux coefficients is tied to the degree of the subspace of spherical harmonics being integrated, $T = N$ and thus $a = b$. With this in mind, we observe that the operator dimensions in the two different formulations are compatible, which facilitates the use of the Exnihilo framework to solve the LDO equations. However, as noted throughout the chapter, the LDO formulation requires particular treatment in several ways when forming and solving the equations.

3.1.4 Scalar Flux

In the traditional formulation of the discrete ordinates equations, the scalar flux is defined as the zeroth moment in the expansion of the angular flux into spherical harmonic functions [2]. In Denovo, it is calculated for a given spatial cell and energy group as

$$\phi = \int_{4\pi} \psi d\mathbf{\Omega} = \sqrt{4\pi} \int_{4\pi} Y_{00}^{e} \psi d\mathbf{\Omega} = \sqrt{4\pi} \phi_{00}^{g}. \tag{3.18}$$

Thus, based on Equation 3.18, Denovo only retrieves the first entry of the angular flux moment storage vector when called upon to calculate the scalar flux.

When solving the LDO equations, the scalar flux is calculated as a weighted sum of the angular flux moments:

$$\phi = \int_{4\pi} \psi d\mathbf{\Omega} = \sum_{n=1}^{N} w_n \psi_n, \tag{3.19}$$

where the weights are those associated with the particular quadrature set and the angular flux coefficients are those values stored in the Denovo flux moment vector. In order to keep the Denovo scalar flux output functionality consistent between LDO quadratures and other quadrature sets, the scalar flux value calculated in Equation 3.19 is multiplied by $\frac{1}{4\pi}$ and written into the first entry of the flux moment storage vector after the calculation has finished.

3.2 Scattering

3.2.1 Matrix Formulation

As mentioned in Chapter 2, the most apparent difference between the standard discrete ordinates equations and the LDO equations is the discrepancy between the two sets of equations' scattering terms. Although the same scattering cross section coefficients are used in both methods when running Denovo, the coefficients are used to construct the scattering terms differently. Recall the operator forms discussed above and consider the following demonstrative example.

Suppose we are considering one spatial cell of a system with two energy groups and a P_1 scattering expansion. It is assumed that particles may scatter between the two energy groups as well as within each energy group. For the traditional discrete ordinates equations, the scattering matrices are

$$[\mathbf{S}]_{0\to0} = \begin{pmatrix} \Sigma_{s0}^{0\to0} & 0 & 0 & 0 \\ 0 & \Sigma_{s1}^{0\to0} & 0 & 0 \\ 0 & 0 & \Sigma_{s1}^{0\to0} & 0 \\ 0 & 0 & 0 & \Sigma_{s1}^{0\to0} \end{pmatrix}, \; [\mathbf{S}]_{1\to0} = \begin{pmatrix} \Sigma_{s0}^{1\to0} & 0 & 0 & 0 \\ 0 & \Sigma_{s1}^{1\to0} & 0 & 0 \\ 0 & 0 & \Sigma_{s1}^{1\to0} & 0 \\ 0 & 0 & 0 & \Sigma_{s1}^{1\to0} \end{pmatrix},$$
$$[\mathbf{S}]_{0\to1} = \begin{pmatrix} \Sigma_{s0}^{0\to1} & 0 & 0 & 0 \\ 0 & \Sigma_{s1}^{0\to1} & 0 & 0 \\ 0 & 0 & \Sigma_{s1}^{0\to1} & 0 \\ 0 & 0 & 0 & \Sigma_{s1}^{0\to1} \end{pmatrix}, \; [\mathbf{S}]_{1\to1} = \begin{pmatrix} \Sigma_{s0}^{1\to1} & 0 & 0 & 0 \\ 0 & \Sigma_{s1}^{1\to1} & 0 & 0 \\ 0 & 0 & \Sigma_{s1}^{1\to1} & 0 \\ 0 & 0 & 0 & \Sigma_{s1}^{1\to1} \end{pmatrix}. \tag{3.20}$$

In contrast, the LDO scattering matrix for within-group scattering in the lower group is

$$[\tilde{\mathbf{S}}]_{0\to0} = \begin{pmatrix} \Sigma_{\mathrm{s},1}^{0\to0}(\boldsymbol{\Omega}_1\cdot\boldsymbol{\Omega}_1) & \Sigma_{\mathrm{s},1}^{0\to0}(\boldsymbol{\Omega}_1\cdot\boldsymbol{\Omega}_2) & \cdots & \Sigma_{\mathrm{s},1}^{0\to0}(\boldsymbol{\Omega}_1\cdot\boldsymbol{\Omega}_N) \\ \Sigma_{\mathrm{s},1}^{0\to0}(\boldsymbol{\Omega}_2\cdot\boldsymbol{\Omega}_1) & \Sigma_{\mathrm{s},1}^{0\to0}(\boldsymbol{\Omega}_2\cdot\boldsymbol{\Omega}_2) & \cdots & \Sigma_{\mathrm{s},1}^{0\to0}(\boldsymbol{\Omega}_2\cdot\boldsymbol{\Omega}_N) \\ \Sigma_{\mathrm{s},1}^{0\to0}(\boldsymbol{\Omega}_3\cdot\boldsymbol{\Omega}_1) & \Sigma_{\mathrm{s},1}^{0\to0}(\boldsymbol{\Omega}_3\cdot\boldsymbol{\Omega}_2) & \cdots & \Sigma_{\mathrm{s},1}^{0\to0}(\boldsymbol{\Omega}_3\cdot\boldsymbol{\Omega}_N) \\ \vdots & \vdots & \ddots & \vdots \\ \Sigma_{\mathrm{s},1}^{0\to0}(\boldsymbol{\Omega}_N\cdot\boldsymbol{\Omega}_1) & \Sigma_{\mathrm{s},1}^{0\to0}(\boldsymbol{\Omega}_N\cdot\boldsymbol{\Omega}_2) & \cdots & \Sigma_{\mathrm{s},1}^{0\to0}(\boldsymbol{\Omega}_N\cdot\boldsymbol{\Omega}_N) \end{pmatrix}. \tag{3.21}$$

The LDO scattering matrices for particle movement between the two energy groups as well as within the higher energy group have been omitted for brevity; these matrices are constructed in the same fashion as Equation 3.21. In this example LDO scattering matrix, a given entry is calculated as

$$\begin{aligned}\Sigma_{\mathrm{s},1}^{0\to0}(\mathbf{\Omega}_n\cdot\mathbf{\Omega}_m) &= \sum_{\ell=0}^{L=1}\frac{2\ell+1}{4\pi}\Sigma_{\mathrm{s},\ell}^{0\to0}P_\ell(\mathbf{\Omega}_n\cdot\mathbf{\Omega}_m)\\ &= \frac{2(0)+1}{4\pi}\Sigma_{\mathrm{s},0}^{0\to0}P_0(\mathbf{\Omega}_n\cdot\mathbf{\Omega}_m)+\frac{2(1)+1}{4\pi}\Sigma_{\mathrm{s},1}^{0\to0}P_1(\mathbf{\Omega}_n\cdot\mathbf{\Omega}_m)\\ &= \frac{1}{4\pi}\Sigma_{\mathrm{s},0}^{0\to0}+\frac{3}{4\pi}(\mathbf{\Omega}_n\cdot\mathbf{\Omega}_m)\Sigma_{\mathrm{s},1}^{0\to0}.\end{aligned} \tag{3.22}$$

Equations 3.20 and 3.21 show several important and distinct differences between the two formulations. In the traditional discrete ordinates formulation, the scattering matrices themselves do not incorporate angular information; they merely hold the constant scattering cross section coefficients. Angular information is incorporated into the system solution via the $\mathbf{M}$ and $\mathbf{D}$ matrices. In contrast, in the LDO formulation, the scattering cross section expansion is contained within the scattering matrix itself. Despite the structural differences, Equations 3.20 and 3.21 employ the same cross section coefficients, as seen in the expansion listed in Equation 3.22.

3.2.2 Cross Section Reconstruction

To demonstrate the formal equivalence of how scattering is handled between the traditional discrete ordinates formulation and the LDO formulation,we present a brief example of scattering cross section reconstruction as a function of angle.

For this example, we will look at the scattering cross section of water at 300 K as a function of $\mathbf{\Omega}\cdot\mathbf{\Omega}'$, the cosine of the outgoing and incoming angles. Here we plot the scattering cross sections for the highest energy group (group 0) of a coarse (8 energy groups) test cross section library distributed with the SCALE software package [3]. A P_3 scattering expansion is used.

In Figure 3.1, we see that the group-to-group cross section with the greatest variation in angle is the downscattering from group 0 to group 1. In the interest of demonstrating how well particular quadrature types reconstruct scattering cross section as a function of angle, we will restrict the following reconstructions to this particular group-to-group cross section. Figure 3.2 shows this cross section reconstructed with the coarsest quadruple range (QR) and LDO quadrature sets available in Exnihilo. The QR quadrature set has one angle per octant and the LDO quadrature set is the "md003.00016" set of ordinates and weights listed in Table 3.1.

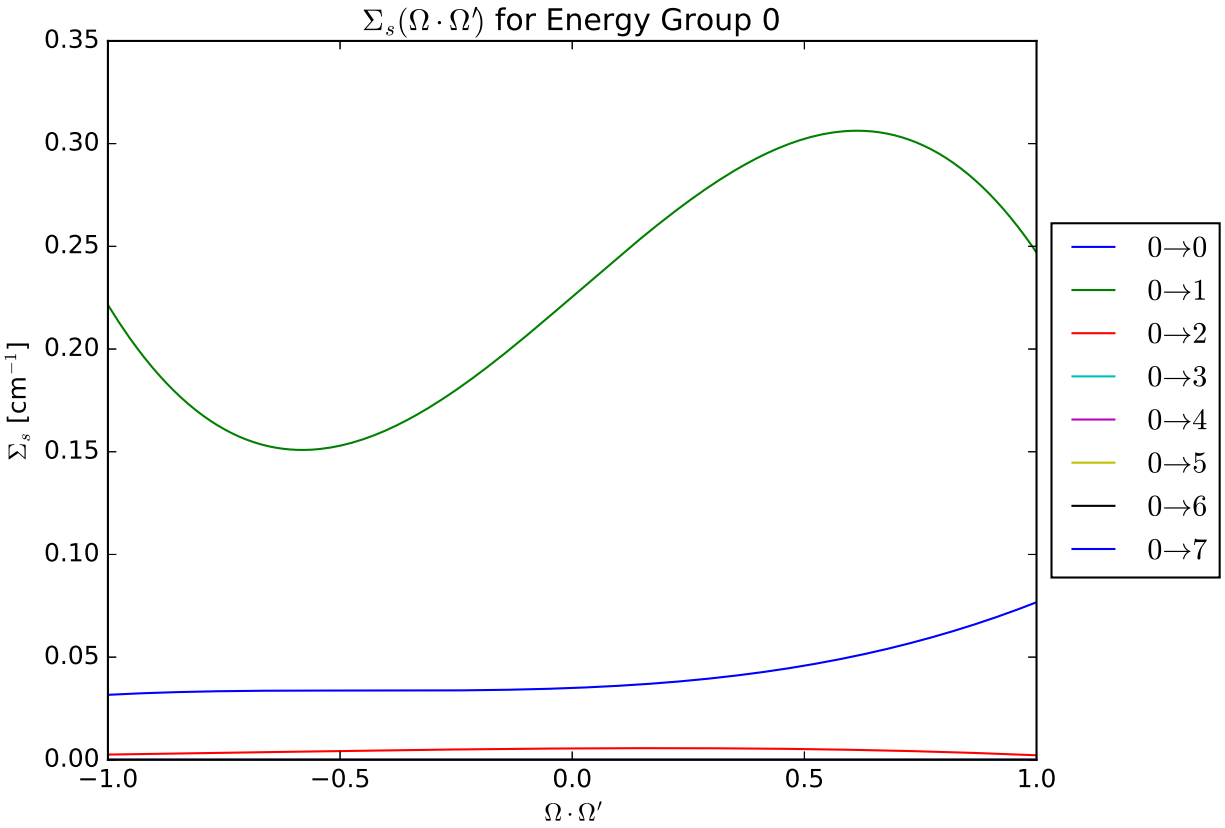

Figure 3.1: Water scattering cross section as a function of angle in the highest energy group.

In Figure 3.2 we see that the coarse QR and LDO quadrature sets both capture the forward-peakedness of this cross section. The QR quadrature set contains fewer unique values of $\mathbf{\Omega} \cdot \mathbf{\Omega}'$ than does the LDO quadrature set, however, and the LDO quadrature set produces values of Σ_s that are closer to the extremal values of the reference cross section curve. The potential impact of this is the possibility of being able to use relatively coarse LDO quadrature sets in solving a problem while incorporating the problem's angular dependence better than a standard quadrature set of a similar coarseness would.

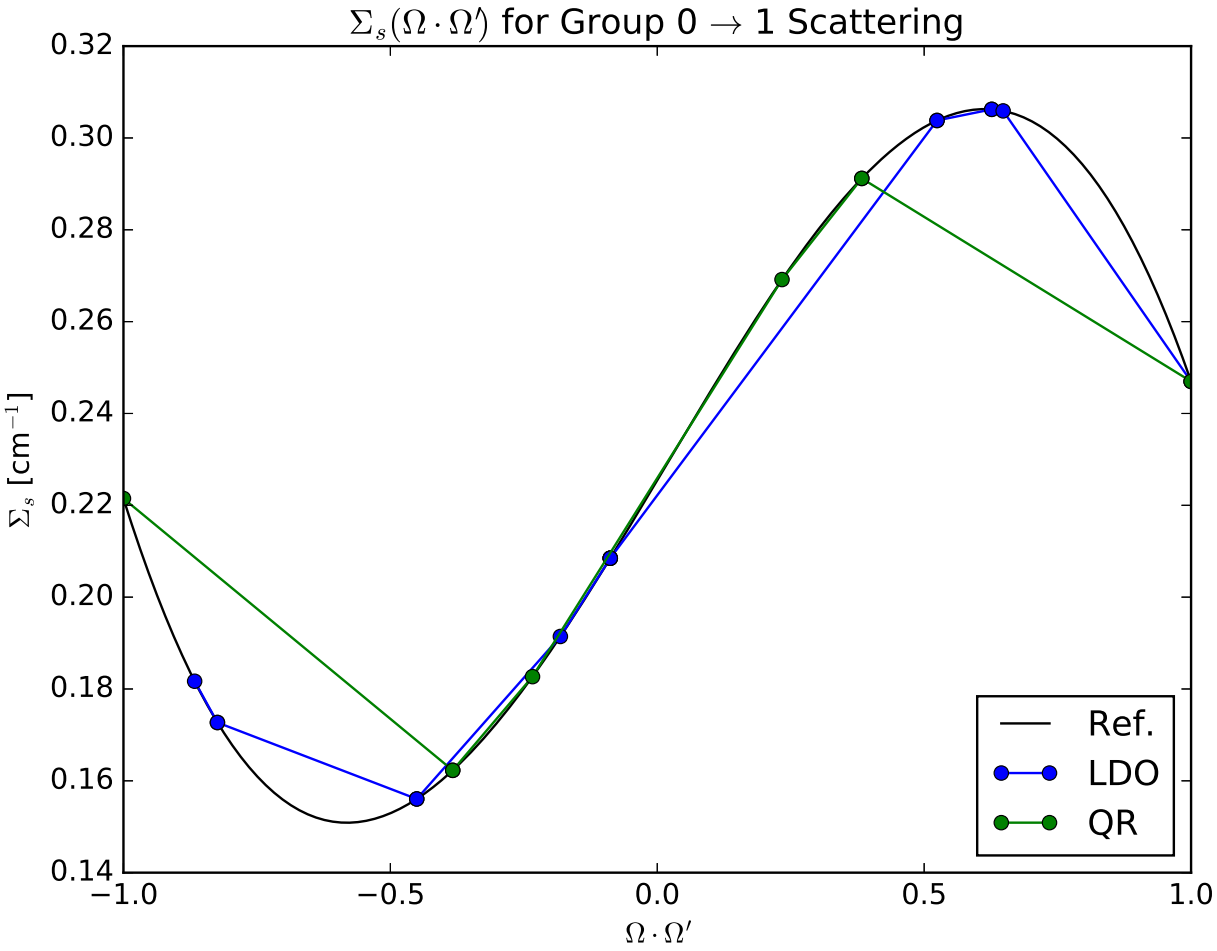

Figure 3.2: Group 0 → 1 scattering cross section reconstructed with coarse angular meshes.

Finer angular meshes of both quadrature set types are shown in Figure 3.3; in this plot the QR quadrature set has 128 angles and the LDO quadrature set has 144 angles. It is seen that both quadrature set types match the reference cross section curve quite well when the angular mesh is refined. This is unsurprising for the QR quadrature set and serves as a confirmation that the LDO formulation is formally the same as the traditional discrete ordinates equations.

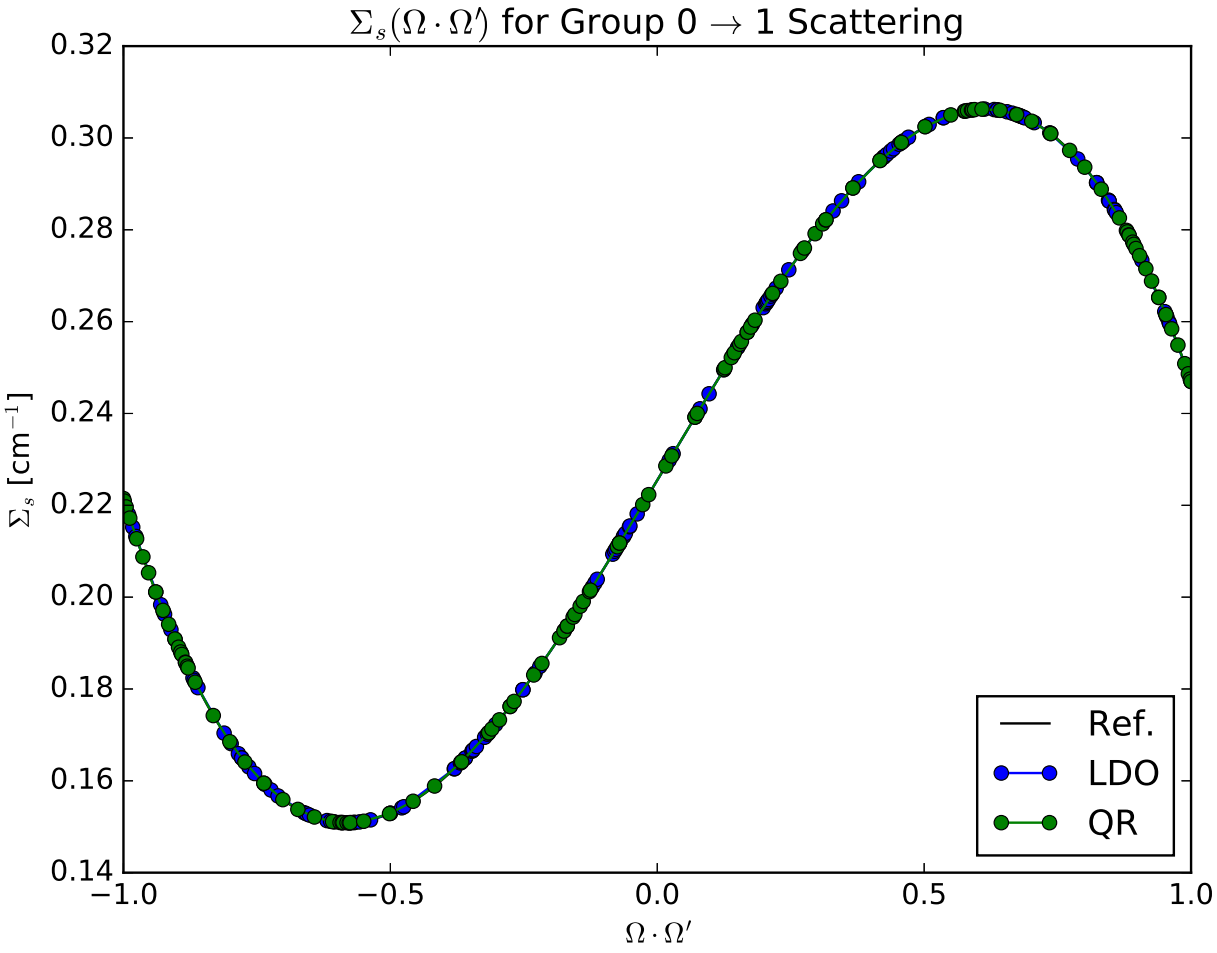

Figure 3.3: Group 0 → 1 scattering cross section reconstructed with fine angular meshes.

3.2.3 Scattering in Denovo

In Denovo and most other discrete ordinates codes, the operation $\mathbf{L}^{-1}$ in Equation 3.3 represents a sweep through the system mesh in the directions of particle travel [4]. We can rewrite Equation 3.3 to reframe it as solving for the total source Q:

$$Q = \mathbf{D}\mathbf{L}^{-1}\left(\mathbf{M}Q_m + Q_d\right). \tag{3.23}$$

Here, the operators are the same as those in Equation 3.3, Q_m is the sum of the "moment-based" sources, and Q_d is the sum of the "discrete" sources [5] as shown in Equation 3.24. Recalling Equation 3.23, moment-based sources are those to which the moment-to-discrete operator $\mathbf{M}$ is applied in the traditional discrete ordinates formulation. Discrete sources are not operated on by $\mathbf{M}$ and may be restricted to a subset of the discrete angles used in a given problem.

$$Q_m = \sum_{s=1}^{S_m} Q_{m,s} \quad \text{and} \quad Q_d = \sum_{s=1}^{S_d} Q_{d,s}, \tag{3.24}$$

where $Q_{m,s}$ is a particular moment-based sweep source, $Q_{d,s}$ is a particular discrete-based sweep source, S_m is the total number of moment-based sources in the system, and S_d is the total number of discrete sources [5]. Figure 3.4 shows the sweep source hierarchy implemented in Denovo, where the goal of the infrastructure is to calculate the total source listed in Equation 3.23 by performing a transport sweep over the combined particle sources.

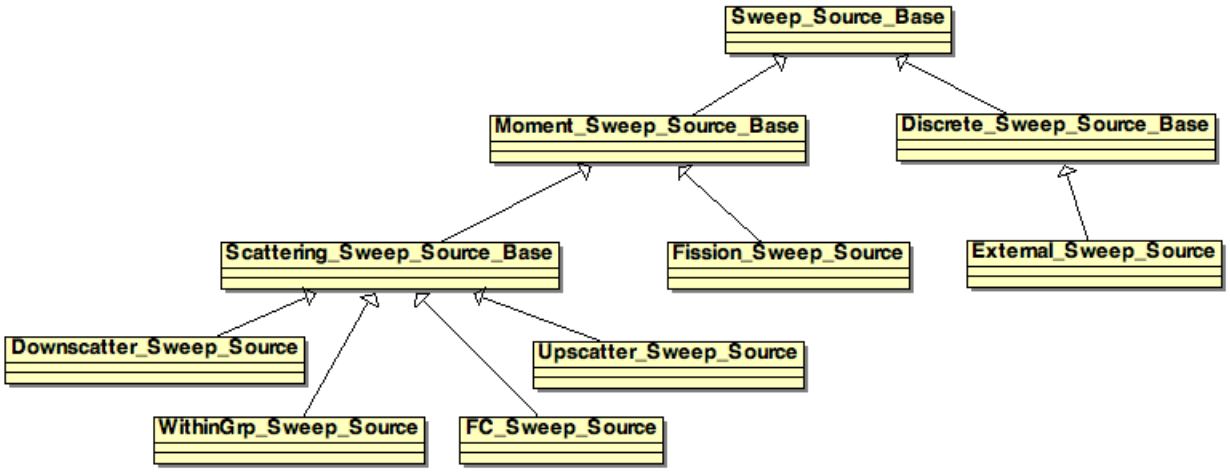

Figure 3.4: Sweep source hierarchy in Denovo [5].

From this diagram, it is apparent that all scattering derives from a common base class, the scattering sweep source base, and that this base class derives from the moment-based sweep source class. The types of scattering supported include downscattering, within-group scattering, upscattering, and first-collision scattering. The scattering classes share a great deal of functionality, hence the implementation of the common base class. Because the scattering sweep source is a type of moment-based sweep source, we note the particular difference in the operator forms of the discrete ordinates and LDO formulations and how that translates into implementing scattering calculations in Denovo.

In the LDO formulation, the interpolation matrix **J** is applied to the moment-based sources. Looking at Equations 3.3 and 3.12, it is apparent that the operator order is different between the traditional discrete ordinates formulation and the LDO formulation, Namely, the product of the scattering matrix and the moment-to-discrete or interpolation matrix is reversed between the two sets of equations. To handle this difference, a "scattering calculator" was implemented in the scattering sweep source base class such that the scattering sweep source is calculated in accordance with the formulation of the equation set being solved.

3.3 Selection of Quadrature Sets

As mentioned in Section 2.3.1, the LDO equations are developed with and must be evaluated at a fundamental system of points for the subspace of spherical harmonics. Ahrens provides references for examples of construction methods of these point systems [6]. Like Ahrens, we have chosen to use the extremal point sets developed and distributed by Womersley [7].

Womersley's extremal systems are generated such that the associated Gram matrix is positive definite [7]; these matrices are of interest to work with from an implementation standpoint because of their low condition numbers. In Table 3.1 we give an example of a point set generated by Womersley. The point set is of degree 3 and thus contains 16 points.

Table 3.1: The "md003.00016" quadrature set developed by Womersley [7].

μ	η	ξ	w
0.00000000000000000	0.0000000000000000	1.0000000000000000	0.73999377643692810
0.89273429807179527	0.0000000000000000	-0.45058348066286125	0.73999377643692787
-0.14301510478336188	0.98579910306911467	-0.088015954189755163	0.73999377643692688
-0.73214276086495222	0.51082433836573149	-0.45058348066286003	0.73999377643692854
0.65748213697787805	-0.7831172071742225	-0.088015954189756496	0.73999377643692765
-0.70626478165373330	0.4595590936077425	0.52407635945553088	0.92161132427900849
-0.60670408850507063	-0.4914548265981833	0.62661538904237324	0.73999377643692887
-0.29492456926406690	-0.9812320737717869	-0.18150577463199227	0.92161132427900960
0.21767572867043725	-0.7831172071742269	0.62661538904237279	0.73999377643692787
-0.51446703219451573	-0.23748738235169115	-0.82396809162048790	0.73999377643692743
0.85155965361038066	-0.013788611344369470	0.52407635945553044	0.92161132427900860
0.28603020956672459	-0.48914548265981850	-0.82396809162048790	0.73999377643692776
0.14962969730741976	0.47595590936077353	-0.86664694427906974	0.92161132427900883
-0.96739492195887000	-0.23748738235169184	-0.088015954189756274	0.73999377643692821
0.68136471239214502	0.72663286501151070	-0.088015954189756274	0.73999377643692898
0.22843682262779150	0.72663286501151014	0.64793618324097579	0.73999377643692754

We note that all of Womersley's extremal systems are generated such that the first point in each set is situated along the z-axis. These systems are rotationally invariant with respect to the maximization of the logarithm of the determinant of the associated Gram matrix, so the point sets may be rotated in space if this vector placement is undesirable for a given scenario. The work presented and discussed in Chapter 4 uses the point sets posted by Womersley; exploration of using rotated extremal point sets is a potential area of future work.

3.4 Restrictions

Several restrictions exist for solving the LDO equations in the Exnihilo framework as well as employing the solutions in the ADVANTG software. Some of these restrictions are a result

of implementing the LDO equations in a framework designed to solve the traditional discrete ordinates equations, while other restrictions are merely current limitations of the software pieces used in this work.

3.4.1 Boundary Conditions

Although it is mathematically possible to use reflective boundary conditions for the LDO equations (given their interpolatory nature), the current implementations of the various codes used in this work restrict the solutions to vacuum (black) boundary conditions at the time of this writing. The primary reason for this is that the ADVANTG software does not support the use of reflective boundary conditions, and the LDO equations were implemented into the Exnihilo framework for the purpose of using the solutions in ADVANTG for Monte Carlo variance reduction parameter generation. To a lesser extent, the Exnihilo framework was built with symmetric quadrature sets in mind, and so the use of reflective boundary conditions with the LDO equations was considered to be an effort beyond the scope of this work.

3.4.2 Uncollided Flux

The use of an "analytic" approximation of the uncollided flux source, a method employed to reduce ray effects from point sources or other small sources [1], is not available when solving the LDO equations through Exnihilo. This approximation is obtained in Denovo by solving the following equations for the group uncollided flux moments for every mesh cell in the calculation domain:

$$\mathbf{\Omega} \cdot \nabla \psi^g(\mathbf{\Omega}) + \Sigma_t^g \psi^g(\mathbf{\Omega}) = \frac{Q_p^g}{4\pi} \delta(r - r_p), \tag{3.25}$$

where $|r - r_p|$ is the geometric distance between the flux source and some particular point and the analytic solution of the above equations is

$$\psi^g(\mathbf{\Omega}) = \delta(\mathbf{\Omega} - \mathbf{\Omega}_{p \to r}) \frac{Q_p^g}{4\pi |r - r_p|^2} e^{-\tau(r, r_p)}. \tag{3.26}$$

In Equation 3.26, the term $\delta(\mathbf{\Omega} - \mathbf{\Omega}_{p \to r})$ indicates that the angular flux at a given point is only nonzero for the the angle that passes directly from the source through the particular point of interest. The "optical path length" $\tau(r, r_p)$ is the integral of the total cross section from the source location to the point of interest and is calculated via ray tracing.

Because the Exnihilo framework was written to solve the traditional form of the discrete ordinates equations, these flux moment solutions in Equation 3.26 are based on the expansion listed in Equation 2.18. That is to say, when using the analytic uncollided flux approximation, the flux moments are calculated using the components of the spherical harmonic functions listed in Equations 2.19 and 2.20. So, the solutions do not apply to the LDO equations and this treatment cannot be used. All tests in the following chapter were run with the

uncollided flux treatment turned off; implementing this approximation for use with the LDO equations in Denovo remains an area of future work.

3.4.3 Particle Sources

When considering neutron transport problems of interest, a small variety of particle source types appear frequently. One typical source type is an isotropic source, in which particles are emitted uniformly in all directions. Specifically, isotropic point sources, in which the physical size of the source itself is negligible, are routinely used in both experimental work and simulations.

Point sources must be approximated as small volumetric sources when solving the LDO equations in Denovo. When a point source is used in a system, Denovo calculates the uncollided flux from that point source using the analytic solution to the NTE. As mentioned previously, this is done to alleviate ray effects. However, as discussed above in Section 3.4.2, these analytic solutions are not applicable when solving the LDO equations. Thus, when a point source is specified in combination with the LDO equations, it is treated as a small volume source instead. In this case, an equal contribution of the source strength is added to every angular flux coefficient in the cell in which the particle source resides. This is notably different from the traditional discrete ordinates formulation in Denovo, in which the source strength is added only to the zeroth flux moment for reasons described in Section 3.1.4.

Finally in this section, we note that this work is limited to isotropic particle sources. At the time of this writing, ADVANTG does not support directional sources [8]; Monte Carlo particle importance maps generated with ADVANTG and Denovo automatically use an isotropic source distribution regardless of the particle source input. Since the ultimate goal of implementing the LDO equations in the Exnihilo framework is to use the results for Monte Carlo variance reduction parameter generation via ADVANTG, implementation of the use of directional sources when solving the LDO equations in Denovo was not pursued in this work.

3.4.4 Fixed Source vs. Criticality Calculations

All scenarios tested in this work are fixed-source problems, though the LDO equations are applicable to k-eigenvalue (criticality) problems in principle. Ray effects, which we are interested in using solutions of the LDO equations to mitigate, largely come from localized sources, as discussed in Section 2.1.2.2. Due to the distributed nature of fission sites in a typical light water reactor, the particle flux in a given criticality calculation will be relatively isotropic and unlikely to incur ray effects within the reactor core. Furthermore, at the time of this writing, ADVANTG only supports generation of Denovo input for fixed-source problems.

Bibliography

[1] Thomas Evans et al. *Exnihilo Documentation: Release 6.2.0 (Dev)*. Tech. rep. Oak Ridge National Laboratory, 2017.

[2] Thomas Evans et al. *Exnihilo Transport Methods Manuals*. Tech. rep. CASL-U-2015-0080-000, Revision 0. Oak Ridge National Laboratory, Mar. 2015.

[3] B. T. Rearden and M. A. Jessee, eds. *SCALE Code System*. ORNL/TM-2005/39, Version 6.2.1. Available from Radiation Safety Information Computational Center as CCC-834. Oak Ridge National Laboratory. 2016.

[4] Thomas M. Evans et al. "Denovo: A new three-dimensional parallel discrete ordinates code in SCALE". In: *Nuclear Technology* 171.2 (2010), pp. 171–200. URL: `https://doi.org/10.13182/NT171-171`.

[5] Greg Davidson and Tom Evans. *Refactoring of Sweep Sources in Denovo (Rev. 3)*. Tech. rep. NMDS-10-004. Oak Ridge National Laboratory, November 28, 2016.

[6] Cory D. Ahrens. "Lagrange Discrete Ordinates: A New Angular Discretization for the Three-Dimensional Linear Boltzmann Equation". In: *Nuclear Science and Engineering* 180.3 (2015), pp. 273–285.

[7] Rob Womersley. *Extremal (Maximum Determinant) points on the sphere S^2*. `http://web.maths.unsw.edu.au/~rsw/Sphere/Extremal/New/index.html`.

[8] Madicken Munk. "FW/CADIS-Ω: An Angle-Informed Hybrid Method for Neutron Transport". PhD thesis. University of California, Berkeley, 2017.